TOXICOLOGICAL SCIENCES **112(1)**, 196–210 (2009)
doi:10.1093/toxsci/kfp195
Advance Access publication August 19, 2009

Investigations of the Use of Bioavailability Data to Adjust Occupational Exposure Limits for Active Pharmaceutical Ingredients

Bruce D. Naumann,*,[1] Patricia A. Weideman,† Ramesh Sarangapani,‡ Shu-Cheih Hu,§ Rakesh Dixit,¶ and Edward V. Sargent||

*Merck & Co., Inc., Whitehouse Station, New Jersey 08889-0200; †Schering-Plough Corp., Kenilworth, New Jersey 07033; ‡Novartis, East Hanover, New Jersey 07936; §IIT Research Institute, Chicago, Illinois 60616; ¶MedImmune, Gaithersburg, Maryland 20878; and ||EV Sargent LLC, Clearwater, Florida 33767

Received April 7, 2009; accepted August 10, 2009

Occupational exposure limits (OELs) for active pharmaceutical ingredients have traditionally been established using no-observed-adverse-effect levels derived from clinical studies employing po and iv routes of administration and by applying default uncertainty factors or chemical-specific adjustment factors. However, exposure by the inhalation or dermal route is more relevant in terms of occupational safety. In this investigation, to explore new methods for route-to-route extrapolation, the bioavailability of MK-0679, a leukotriene D_4 receptor antagonist, was compared following iv, po, intranasal (in), or intratracheal (it) administration. The relative bioavailability of MK-0679 was iv ≅ it > po ≅ in. Bioavailability correction factors (BCFs) of 2.0 and 0.6 were derived from these data to adjust a hypothetical OEL of 0.1 mg/m^3 for MK-0679 with particle sizes of 10 and 50 μm, respectively. These BCFs were used to adjust the OEL established using po clinical data, to reflect the differences in bioavailability following deposition in different regions of the respiratory tract. To further investigate how bioavailability data could be used in setting OELs, a preliminary pharmacokinetic (PK) model was developed to describe the time course of plasma concentrations using the data from the route comparison study. An inhalation study was then performed to test the validity of using either empirical data or modeling approaches to derive BCFs when setting OELs. These investigations demonstrated how the use of route-specific PK data could reduce some of the uncertainties associated with route-to-route extrapolation and allow for improved precision and quantitative adjustments when establishing OELs. Further investigations are needed to better understand the factors responsible for differences in systemic uptake following deposition in different regions of the respiratory tract and how these can be generalized across different classes of soluble compounds.

Key Words: **absorption; bioavailability; OEL; pharmaceutical; respiratory tract.**

Occupational exposure limits (OELs) are used by pharmaceutical companies to provide guidance for acceptable levels of occupational exposure to the active pharmaceutical ingredients (APIs) used in products that, by design, are biologically active. Typically, the OEL for an API is established by dividing the no-observed-adverse-effect level (NOAEL) for the most sensitive pharmacological or toxicological end point by appropriate uncertainty factors. Additional adjustments may be made on the basis of available pharmacokinetic (PK) data (e.g., steady-state levels and bioavailability data; Naumann and Weideman, 1995; Sargent and Kirk, 1988). The NOAEL is generally determined by the use of animal and/or human data obtained following exposure to a drug via the traditional clinical routes of iv or po administration. Administration of a drug by the iv or po route provides information on the safety, efficacy, and PK of the drug in patient populations; however, for application to the workplace, it is then necessary to extrapolate these data to the inhalation route. In the absence of this information, it is generally assumed that 100% of the inhaled mass is deposited in the respiratory tract and completely absorbed. Although dermal contact may also contribute to workplace exposure for certain compounds, the current investigation focused only on the inhalation route.

Adjustment of OELs on the basis of differences in bioavailability occurs infrequently mainly because appropriate data are not generally available to support quantitative adjustments. This study illustrates how generation of bioavailability data could provide a scientific basis for compound-specific adjustments to the OEL. By knowing the differences in bioavailability (and therefore systemic exposure) between the clinical route used as the basis for the OEL and occupationally relevant route(s), there is greater confidence that the resulting OEL will provide adequate protection.

The best way to derive a bioavailability correction factor (BCF) for a particular chemical is to perform a PK study using the primary relevant route of exposure for workers (i.e., inhalation) and to compare the area under the plasma concentration versus time curve with similar data for the clinical route of exposure (e.g., po) on which the OEL is based. However, due to the relatively high cost and complexity of inhalation studies, there is an interest in being able to estimate an inhalation BCF from surrogate data, e.g., intranasal (in) and intratracheal (it) instillation data. The preliminary

[1] To whom correspondence should be addressed at Merck & Co., Inc., Two Merck Drive, WS2W-18, Whitehouse Station, NJ 08889-0200. Fax (908) 735-1496. E-mail: bruce_naumann@merck.com

investigations reported here were conducted to determine whether this alternative BCF approach would be viable. Initially, an experiment was performed to compare the time course of plasma concentrations following administration by different routes of exposure. This investigation also explored the feasibility of using a PK modeling approach to predict systemic exposures following inhalation of pharmaceutical aerosols, which are relatively soluble particles compared with many workplace dusts. If successful, it might be possible to derive bioavailability adjustment factors without performing any animal testing. An inhalation study was performed to determine if the alternative testing or modeling approaches had validity.

Pharmaceutical companies are interested in delivering drugs via the respiratory tract to take advantage of the large surface area and thinness of the air-blood barrier. However, the depositional characteristics and physicochemical properties of APIs remain problematic, and special efforts must be made to ensure reproducible and sufficient delivery of drug (Scheuch *et al*., 2006). PK models have been developed to define absorption and disposition of specific drugs (Gopalakrishnan *et al*., 2005; Krishnaswami *et al*., 2005), but no methods are available to develop quantitative data to account for differences in bioavailability from the respiratory tract to support OEL setting. Much more work has been done for volatile compounds. For example, a model was developed that combined computational fluid dynamics with physiologically based pharmacokinetic (PBPK) modeling to define the nasal dosimetry in support of risk assessments for acrylic acid (Andersen *et al*., 2000). Similar work with methyl methacrylate and vinyl acetate demonstrate how having a better understanding of key aspects of tissue interactions, whether deposition, absorption, local alterations in pH, and metabolism, can enhance risk assessments (Andersen *et al*., 2002). The current study embraces this scientific approach of combining information on local deposition and disposition to inform the risk assessment for soluble aerosols.

Specifically, the experimental design in these investigations was developed to evaluate how the apportionment of deposition and absorption in each region of the respiratory tract could influence resulting plasma concentrations. If successful, it could provide a basis for extrapolating from the po to the inhalation route of exposure and permit the derivation of a BCF for use in setting OELs. The results of the route comparison study, first reported in preliminary form by Weideman *et al*. (1997), were used to develop a preliminary PK model to describe systemic exposure following inhalation of a soluble pharmaceutical aerosol. The model was then tested with an inhalation PK study employing two different particle sizes to maximize deposition in either the upper respiratory tract (URT; comprising the nasopharyngeal region) or the lungs (comprising the tracheobronchial [TB] and pulmonary [PU] regions). MK-0679, a leukotriene D_4 receptor antagonist discontinued from development for treatment of asthma, was used in these investigations. The ultimate goal of these investigations was to evaluate whether differences in bioavailability could serve as the basis for the derivation of BCFs for making appropriate adjustments to OELs for active pharmaceutical ingredients and to encourage further investigations in this area.

MATERIALS AND METHODS

Chemicals

MK-0679, a leukotriene D_4 antagonist, was used in these experiments. It is chemically known as (R)-5-(3-(2-(7-chloroquinolin-2-yl)ethenyl)phenyl)-4, 6-dithianonanediote-N,N-dimethyl amide carboxylic acid, sodium salt (Lot 020), and was obtained from Merck & Co., Inc. (Whitehouse Station, NJ). 1-(((1R-(3-(2-(7-chloro-2-quinolinyl)-(E)-ethenyl)phenyl)3-(2-(1-hydroxy-1-methylethyl) phenyl)propyl)-thio)-methyl)isopropane), sodium acetate (Lot 001), was used as an internal standard and was also obtained from Merck & Co., Inc. Acetonitrile (omnisolve grade) and methanol (omnisolve grade) were purchased from EM Science (Gibbstown, NJ; route comparison study) or Fisher Scientific (Houston, TX; high performance liquid chromatography [HPLC] grade in inhalation study). Forane (isoflurane) was obtained from Ohmeda, Inc. (Liberty Corner, NJ). *o*-Phosphoric acid (85%; HPLC grade) and triethylamine (peptide synthesis grade) were purchased from Fisher Scientific (FairLawn, NJ). PBS, without Ca, Mg(PBS−), pH 7.4, and sodium bicarbonate solution 1.25% were obtained from GIBCO (Grand Island, NY).

Animals and Handling

For the route comparison study, young, adult male Sprague-Dawley rats were obtained from Charles River Laboratories, Inc. (Raleigh, NC). Rats were 7–9 weeks of age at dosing (225–325 g). Food was provided *ad libitum* for the duration of the study, with the exception of 18-h pre-dose and 4-h post-dose for all routes of exposure. Water was provided *ad libitum* throughout the study. Animals were housed individually in hanging wire-meshed cages prior to dosing. After dosing, animals were pair housed in plastic nesting boxes containing cedar shavings until sampling time points.

For the inhalation study, 67 male Sprague-Dawley (Crl:CD[SD]IGS BR) rats were purchased from Charles River Labs (Portage, MI). The rats were 7 weeks old at the time of receipt. The rats were quarantined for at least 8 days before they were exposed to the test atmosphere. At the time of exposure, the body weights (BWs; mean ± SD) for two inhalation exposure groups were 281 ± 13 and 299 ± 9 g, respectively. Throughout the duration, rats were double housed, when possible, in stainless steel cages suspended over absorbent paper cage boards. The cages were equipped with automatic drinking water supply systems and feeders. The food (Certified Rodent Diet/Meal 5002; PMI Nutrition International, Inc. (Brentwood, MO) and water (City of Chicago Municipality water) were administered *ad libitum* during nonexposure periods. Environmental conditions including room temperature (19.0°C–23.9°C), relative humidity (37.8–79.7%), and light cycle in the animal rooms were monitored daily.

Plasma Sample Analyses

In the route comparison study, test samples (100 µl) were prepared by adding 50 µl of 50:50 methanol/water and 50 µl of the working internal standard solution. Plasma standards of MK-0679 were prepared by adding 50 µl of the MK-0679 working standard to 100 µl of control rat plasma, followed by 50 µl of the working internal standard solution. Acetonitrile (200 µl) was added to the samples and standards to precipitate protein. The contents were vortexed and centrifuged at 21,000 × g for 5 min at 4°C. The supernatant (300 µl) was diluted with 0.1% H_3PO_4/0.1% triethylamine solution (200 µl) and injected onto the HPLC system. The ratios of MK-0679 to the internal standard areas were determined. The standard curve for the weighted

TABLE 1
Route Comparison of the PK of MK-0679. Plasma Concentrations for C_{max}/Dose and $AUC_{0\text{-}6h}$/Dose Are Shown with the Mean ± SE

PK parameter	Route of administration			
	iv	it	po	In
Dose (mg/kg)	10	12.5	100	12.5
T_{max} (h)	0.08	0.08	1	0.25
$t_{1/2}$ (h)	1	1.1	3.7	2.5
C_{max} (ng/ml)	35,175	87,533	38,692	3540
C_{max}/dose	3518 ± 718	7003 ± 1349	387 ± 161	283 ± 55
$AUC_{0\text{-}6h}$ (ng·h/ml)	27,074	46,750	110,963	8356
$AUC_{0\text{-}6h}$/dose	2707 ± 219	3740 ± 360	1110 ± 170	669 ± 71
n	6	6	6	6

(1/concentration) peak area ratio versus concentration was determined using linear regression. The concentration of MK-0679 in each unknown sample was calculated from the standard curve. Analyses were performed in Merck's Safety Assessment laboratories.

In the inhalation study, 0.1 ml of the plasma layer from chilled centrifuged blood samples, were transferred to a 1.5-ml, amber microcentrifuge tube with 0.3 ml of acetonitrile (HPLC grade; Fisher Scientific, Houston, TX). Samples were centrifuged at 3000 × g for 5 min; the unused plasma samples were stored at –70°C. After centrifugation, the supernatant layer samples were transferred to a disposable autosampler amber microvial and analyzed by HPLC (Waters Alliance 2690; Waters Co., Milford, MA). The detection limit for the analytical method was estimated to be 0.10 μg of MK-0679/ml of plasma.

Filter Analysis

Each filter used to characterize chamber concentrations was extracted with 30 ml of methanol for 60 min in an ultrasonicator and analyzed quantitatively by HPLC (Waters Alliance 2690; Waters Co.).

Route Comparison Study

Study design. Young, adult male Sprague-Dawley virus antigen–free rats were given single iv, it, po, or in doses (mg/kg BW) of MK-0679. Rats were unanesthetized for po and iv dosing and were induced to a lightly anesthetized state with inhaled isoflurane for it and in dosing. Whole blood samples were collected via cardiac puncture from CO_2-euthanized rats (six rats/route/time point) at discrete time points after exposure and plasma fractions were analyzed to determine the bioavailability of drug. Areas under the plasma concentration versus time curve ($AUC_{0\text{-}6h}$) were determined for each route. Data were analyzed using multiroute comparisons of $AUC_{0\text{-}6h}$ and C_{max} (normalized to dose) with the use of a Bonferroni correction. Significance was established at $p < 0.05$.

In a separate experiment to evaluate the potential inflammatory response and its effect on lung pathology, rats were given single it or in doses of MK-0679 or vehicle (PBS−). At 4 and 24 h post-dose, the rats (three rats/route/time point) were killed and underwent bronchoalveolar lavage (BAL) of the right lung or nasal lavage (NL). BAL fluid (BALF) or NL fluid (NLF) was examined for total protein content, total cell count, and underwent differential analysis. The lungs of the it dosed rats were excised, fixed, and examined microscopically for gross pathological changes.

Dosing procedures. Doses, dosing volumes, type of anesthesia, and sample collection times are given in Table 1. Doses were chosen based upon those iv and po doses used in previous preclinical studies using MK-0679. Doses for it and in delivery were chosen based upon the ability to formulate adequate doses based on animal BW and appropriate dosing volumes for these routes of exposure. Six rats/route/time point were used for the collection of plasma samples, and three animals/route/time point were used for the lavage portion of the study. Rats were observed for signs of toxicity throughout the post-dose intervals.

Dosing solutions. Dosing solutions were prepared fresh daily. MK-0679 was prepared in 1.25% sodium bicarbonate solution for iv administration. Dosing solutions for po, it, and in administration were prepared in PBS− (pH 7.4). Solutions for iv, it, and in dosing were sterilized through a 0.22-μm filter prior to administration. Dosing volumes and doses (mg/kg BW) were adjusted using the animal's BW obtained immediately prior to dosing. All lavage procedures used PBS−.

Oral. Unanesthetized rats were given 100 mg/kg BW (5 ml/kg BW) via a ball-tipped, 18-gauge gavage needle attached to a syringe. The tip of the gavage needle was wiped prior to administration of test article to each animal.

Intravenous. Unanesthetized restrained rats were given 10 mg/kg BW (1 ml/kg BW) via the tail vein using sterile tuberculin syringes and needles (25 gauge) and aseptic technique.

Intratracheal. Anesthetized rats were given 12.5 mg/kg BW (≈100 μl total volume/rat) of test material. Animals given vehicle for lavage experiments received ≈100 μl total volume of PBS− based on animal weight. Rats were individually anesthetized prior to it instillation of the test material with a constant flow of 5% Forane (isoflurane). Using a modified, lighted, pediatric laryngoscope, the larynx was visualized, and a blunted, curved, 18-gauge stainless steel catheter attached to a sterile, prefilled syringe was advanced into the trachea to the carina at the beginning of an inspiration, withdrawn approximately 1 mm, and the test material was instilled briskly into the lungs.

Intranasal. The in dose of MK-0679 was 12.5 mg/kg BW, which was divided into two equal volumes of ≈50 μl/nare for a total volume of ≈100 μl/rat. Control animals given vehicle for lavage experiments similarly received ≈100 μl total volume of PBS− based on animal weight. Rats were anesthetized using the same procedure as that for it instillation. Using a micropipettor, a droplet of dosing solution was gently placed at the opening of the nare with the pipette tip. As the rat began an inspiration, the droplet was completely aspirated. The same technique was repeated for the other nare.

Sample collection. Whole blood samples were obtained by cardiac puncture from CO_2-euthanized rats 5, 15, 30, and 45 min and 1, 2, 4, 6, and 24 h post-dose. Blood was collected into 5-ml Vacutainer tubes containing EDTA (Becton-Dickinson, Rutherford, NJ). Whole blood was kept chilled on ice until centrifugation at 1600 × g for 10 min at 20°C. The plasma layer was collected and stored at −70°C until analysis. BAL or NL was performed on naive rats (no vehicle or test material), and vehicle- or test material–treated rats at 4 and 24 h post-dose. Animals that underwent BAL or NL were killed by lethal injection (ip) of sodium pentobarbital (150–250 mg/kg), followed by thoracic puncture and exsanguination. For BAL, the trachea was exposed by blunt dissection and a blunted 18-gauge stainless steel catheter inserted in a caudal position into a tracheotomy and secured with a suture. The right lung only was isolated and lavaged with three 3-ml volumes of sterile PBS− at room temperature; the first lavage volume was retained separately for total protein content determination. Upon completion of the lavage, both lungs were infused with 10% formalin, removed from the thoracic cavity, and stored in 10% formalin for pathological examination. For NL, the trachea was exposed by blunt dissection and a blunted 18-gauge stainless steel catheter attached to a sterile syringe prefilled with PBS− (1 ml) inserted cranially into a tracheotomy. The catheter was held in place by gentle manual pressure during the lavage procedure. NLF was collected gravimetrically into sterile polypropylene tubes.

Cell counts and lavage fluid. The BALF or NLF was centrifuged at 400 × g for 15 min at 4°C. Acellular supernatant (first BAL volume only; total NL volume) was stored at −70°C until analysis for total protein content. Cell pellets from three BAL volumes or single NL volume were resuspended in PBS− and counted using a hemocytometer. Cell viability was determined using trypan blue exclusion. Differential slides were stained with hematoxylin and

eosin and examined microscopically. Total protein content of the acellular lavageates was determined using bicinchoninic acid.

Lung tissue preparation. A 3-mm-wide section from the hilus to the margin following the major bronchus was taken from the left diaphragmatic and right lung lobes of the formalin-fixed lungs. Tissues were processed and stained with hematoxylin and eosin for microscopic examination.

Statistical analysis. Plasma data were analyzed using multiroute comparisons of C_{max} and $AUC_{0\text{-}6h}$ (normalized to dose) with the use of a Bonferroni correction (Hsu, 1996). Normalized values were used because of the different doses of test material used in the study for each route. Significance was established at $p < 0.05$. However, in order to achieve an overall p value of less than 0.05 for all six comparisons using the Bonferroni correction, only p values less than 0.008 (0.05 divided by 6) were claimed to be significant at the 5% level. Statistical analyses of the cell count and total protein data were not performed due to the limited sample size.

Inhalation PK Study

The final phase of these investigations was an inhalation PK study conducted with MK-0679 to test of the feasibility of using surrogate (in/it) dosing and/or the preliminary model to estimate systemic exposures following inhalation. This represented an initial verification of the proposed approach for deriving BCFs to address route-to-route extrapolation when setting OELs.

Study design. Two groups (groups 1 and 2) of young, adult male Sprague-Dawley rats were exposed to test atmosphere containing aerosols with mass median aerodynamic diameter (MMAD) of either 1.4-μm (group 1) or 3.5-μm (group 2) MK-0679 aerosol at a target concentration of 100 mg/m^3 for 1 h (i.e., 6 mg/kg BW). Each group of animals was divided into six subgroups of five animals, and blood samples were collected, via cardiac puncture, from one designated subgroup at 15, 30, 60, 120, 240, or 360 min postexposure. Plasma fractions were analyzed by means of HPLC for the determination of the concentration of MK-0679. Thirty animals were randomly assigned (group 1) by means of a computer program (RANSD.BAS [EXE], version 1.0), which performed a constrained randomization process based upon the BWs. The remaining animals were weighed and randomized and another 30 animals were assigned to group 2. All animals selected for the inhalation exposure study were identified by ear tagging, a unique permanent identification number.

Inhalation exposures. The study was conducted using a 210-l nose-only inhalation exposure chamber at the Illinois Institute of Technology Research Institute. The exposure chamber provided a uniform and continuous stream of fresh test atmosphere passing the noses of animals. Animals were held in clear plastic restraining tubes (CH Technologies, Westwood, NJ) throughout the exposure duration to minimize whole body exposure and to maximize PU exposure. Airflow to the exposure chamber was maintained at 35 liters per minute (10 air changes per hour) for both exposure groups, and the oxygen level in the chamber ranged from 20.2 to 21.1% throughout the exposure duration. The exhaust from the exposure chamber flowed through a high efficiency particulate air filter and was subsequently exhausted outside the building by means of a blower. Test atmosphere temperatures (mean ± SD) were 20.7 ± 0.79°C and 22.9 ± 1.07°C for exposure groups 1 and 2, respectively; relative humidity values (mean ± SD) were 98.3 ± 0.76 and 96.9 ± 1.07%, respectively.

Test atmospheres were generated by spraying the test article solution into a drying chamber by means of an air atomizing nozzle (Model 1/4J; Spraying System Co., Wheaton, IL) with filtered compressed air. Test article solution was prepared fresh daily by dissolving MK-0679 in PBS. Solutions of 1.1% and 17.9% (wt/wt) were used to generate the aerosols with MMADs of 1.4 and 3.5 μm, respectively. The measured MMADs (mean ± SD) were 1.4 ± 0.07 and 3.5 ± 0.23 μm with mean geometric SDs (GSDs) of 2.4 and 2.0 for exposure groups 1 and 2, respectively. Larger particle sizes could not be generated due to foaming that resulted from the surfactant properties of the test material. The mass concentration of MK-0679 aerosols generated for 3.5-μm-size aerosol was significantly higher than that for 1.4-μm-size aerosol. In order to keep the test atmosphere concentration similar for both groups, an exhaust bypass was installed prior to the entrance of exposure chamber.

The MK-0679 aerosol mass concentration was determined at the breathing zone of the rats at least twice during the exposure period. Aerosol samples were collected on pre-weighed glass fiber filters (1-μm porous size; PALL, Ann Arbor, MI) placed in plastic filter holders with a constant flow rate provided by an appropriate vacuum pump. A dry gas meter connected to the pump was used to measure the corresponding total volume of chamber air sampled. The aerosol concentration in the exposure chamber was determined by HPLC and also continuously monitored by means of a real-time back-scattering aerosol sensor. The particle size distribution of MK-0679 aerosol was determined three times during the exposure duration using a quartz crystal microbalance (QCM)–based 10-stage cascade impactor (California Measurements, Sierra Madre, CA). The QCM sampled at a rate of 0.24 l/min, separating the aerosol particles into 10 sequential aerodynamic size ranges from 0.07 to 35.4 μm. MMADs and GSDs were determined from the mass accumulated on each stage of the QCM.

Plasma samples. Upon termination of inhalation exposure, blood samples were collected, via cardiac puncture, from one designated subgroup each at discrete time points of 15, 30, 60, 120, 240, or 360 min postexposure (i.e., five rats/time point) for the determination of drug bioavailability. Animals were anesthetized by inhalation of 30% CO_2/70% air. Within 5 min of termination of exposure, samples of approximately 3 ml of blood were collected into 4-ml Vacutainer tubes containing EDTA (Becton-Dickinson, Franklin Lakes, NJ) and chilled on ice until centrifugation at 210 × g for 10 min at room temperature before being prepared for analysis by HPLC.

Data analysis. The exposure dose (mg/kg BW), shown in the equation below, was calculated from the aerosol mass concentration (C_m; mg/m^3) in the exposure chamber, mean BW (W_{BD}; kg) of each exposure group, a nominal minute ventilation of 250 ml/min, and an exposure duration of 1 h (volume inhaled = 0.015 m^3).

$$\text{Exposure dose} = C_m \times 0.015 / W_{BD}.$$

Normalized MK-0679 concentrations in plasma were calculated by dividing the plasma concentrations by the respective exposure dose levels, and the comparison of the normalized plasma concentrations between the two exposure groups was analyzed by t-test at each discrete time point. Area under the curve of mean normalized plasma concentrations between 0 and 6 h postexposure ($AUC_{0\text{-}6h}$) was computed using the trapezoidal rule. The maximum normalized plasma concentration (C_{max}), its corresponding postexposure time point (T_{max}), and half-life ($t_{1/2}$) were obtained from the smoothed (spline) curve of mean normalized plasma concentration with respect to postexposure time (SigmaPlot, version 8.0; SPSS, Inc., Chicago, IL).

The potential differences in bioavailability of MK-0679 following inhalation exposure were assessed using two distinct particle sizes to deliver those particles preferentially into different regions of the respiratory tract. In order to do this, the exposure doses needed to be corrected for the aerosol deposition efficiency of the two particle sizes. Raabe *et al.* (1977, 1988) measured PU deposition of inhaled particles in rats using monodisperse aerosols with sizes ranging from 0.2- to 10-μm-diameter particles. Using the deposition efficiencies for the particles used in this study, the total respiratory tract deposition increased from 36 to 85% for 1.4- and 3.5-μm-size particles, respectively. The URT deposition increased from 22 to 73%, respectively. The deposition fraction in thoracic region (TB + PU) remained relatively constant (12–14%), ranging from 5 to 7% in both TB and PU regions. Because deposition dose and site may play an important role in determining the bioavailability of inhaled aerosols, the delivered dose to the respiratory tract and normalized PK parameters with respect to the delivered dose were estimated using the following equation:

$$\text{Delivered dose} = \text{exposure dose} \times \% \text{ deposition}.$$

PK Model Development

Using the data from the route comparison study, a simple PK model was developed to predict the plasma concentration time course for drugs administered via the iv, po, in, and it routes. The model consists of

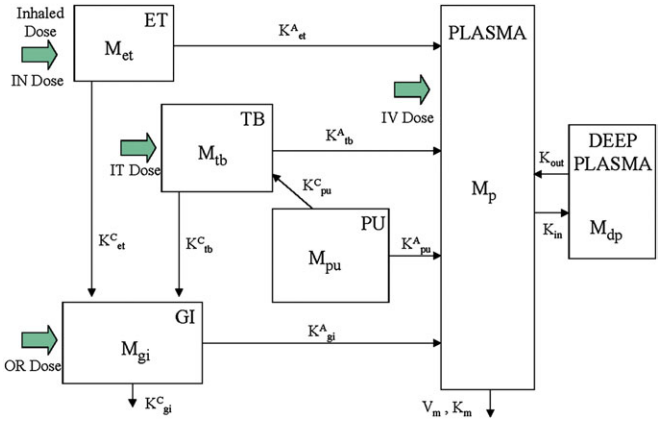

FIG. 1. A general multiroute, multicompartment PK model for drug disposition. *Note*. Rate constants K^A_{tb} and K^C_{pu} were set to zero to provide the best fit for MK-0679.

a multicompartment respiratory tract linked to a gastrointestinal (GI) tract compartment and a systemic blood compartment (Fig. 1). A second, deep compartment, representing volume of distribution and tissues (e.g., adipose) that can store the compound, was added to the systemic model due to the biphasic nature of the iv data for the chemical being modeled. Drug administered via the iv or the po route was modeled as a bolus input to the blood or GI tract compartment, respectively. Drug administered via the in or the it route was modeled as a bolus input to the appropriate respiratory tract compartment(s).

Respiratory tract structure. The respiratory tract of humans, as well as other animals, can be broadly divided into three regions based on structure and function: the extrathoracic region (ET) that extends from the external nares to the larynx, the TB region that includes the trachea and conducting airways extending down to the terminal bronchioles, and the PU region that includes the terminal bronchioles and alveolar sacs. The deposition, clearance, and absorption mechanisms are different in these three regions. The reference concentration dosimetry guidelines (EPA, 1994) partition the lung into three subcompartments to represent the ET, TB, and PU region. A similar lung compartmentalization is used in the model developed for this investigation. The thoracic (lung) region comprises the TB and PU regions.

Respiratory tract deposition. Inhaled particles deposit in one of the three regions depending on the aerosol size, breathing characteristics, and airway morphometry. Empirical relations are available to estimate the regional deposited fraction of inhaled aerosols (EPA, 1994; James *et al*., 1991). However, no such analytical method is available to compute the deposited fraction for aerosolized drugs administered via the in and the it routes. In this investigation, it was assumed that aerosols administered via the in route are completely deposited in the ET region (URT). In the case of it administration, however, deposition can occur in both the TB and the PU regions (i.e., the thoracic region). In this investigation, it was assumed that the instilled compound was deposited in both the TB and the PU regions. The regional deposited fraction was then estimated based on the resulting agreement of the model with the experimental data for systemic uptake.

Respiratory tract clearance. After deposition in the lung, the inhaled particles either dissolve in the airway fluid and are absorbed into the systemic circulation or are physically cleared. The rate of dissolution of the aerosolized drug in the airway fluid is influenced by the aerosol surface to volume ratio, its chemical composition, and other surface properties of the aerosol (Mercer, 1967; Morrow, 1973). The undissolved portion of the aerosol is cleared from the airway by physical transport processes. The rate of clearance depends on the site of deposition in the respiratory tract. Particles depositing on the ciliated portion of the posterior ET region are removed by the rapid mucociliary clearance toward the oropharynx, where they are swallowed (Hinchcliffe and Illum, 1999). The current ICRP (1994) lung model uses a half-time of 10 min for particles depositing in this region. Particles deposited in the nonciliated anterior nasal region are removed by extrinsic means (e.g., nose blowing, wiping) with an assumed half-time of 17 h.

Particles depositing in the TB region are cleared from the airways via the mucociliary escalator into the oropharynx, where they are also swallowed. Lung clearance experiments using radiolabeled aerosols indicate a biphasic clearance rate: a fast phase completed within 24–48 h that has been generally attributed to TB clearance and a slow phase attributed to clearance from the PU region (Roy, 1989). The ICRP lung model uses a half-time of 100 min for particle transport in the conducting airways of the lung. Clearance half-times from the alveolar region are on the order of days to years depending on the solubility (or lack thereof) of the deposited material. The relatively slow clearance rate from the TB and PU regions allows greater opportunity for solubilization. Most pharmaceuticals would be considered relatively soluble materials (compared with many workplace dusts) and would not be expected to persist in the lung for extended periods of time (i.e., residence time of minutes to hours rather than days to years).

In general, the impact of mucociliary transport becomes insignificant for compounds that dissolve rapidly compared with the half-time of mucociliary transport. Brown and Schanker (1983) reported absorption half-times ranging from 0.25 to 34.5 min for 12 drugs following inhalation or it instillation. In this investigation, simple first-order clearance rates were used in the three respiratory tract compartments; these rate constants were estimated from fitting of the available experimental data.

Respiratory tract absorption. The systemic availability of substances dissolved in the airway lining depends on tissue permeability, regional blood perfusion rate at the site of absorption, and enzymatic degradation in the airway epithelium. The airway permeability is determined by parameters such as molecular weight, lipid solubility, water solubility, partition coefficient, and the thickness of the airway epithelium (Widdicombe, 1998). Pulmonary absorption studies using both it-instilled aerosols and inhaled aerosols in mouse, rabbit, and rat have demonstrated first-order kinetics for the absorption process (Schanker *et al*., 1986). Therefore, in this investigation, a first-order absorption rate into the plasma from each of the respiratory tract subcompartments has been assumed, and the values for these rate constants have been estimated using the experimental data.

Systemic uptake and clearance. Chemical reaching the GI tract (transported into the GI tract through mucociliary clearance, administered orally, or administered via enterohepatic recirculation) is absorbed systemically with an absorption rate depending on the po bioavailability of the drug. In this investigation, the absorption process in the GI tract was modeled using first-order kinetics. Chemical that is not absorbed in the GI tract is eliminated into the feces with a first-order clearance rate. These rate constants are determined by optimizing model predictions to fit the experimental data. Chemical reaching the blood compartment (from the lung, GI tract, or administered iv) is cleared from the systemic circulation depending on the properties of the drug. For this preliminary investigation, an empirical two-compartment systemic model was used; however, a more complete PBPK description could be used if adequate data were available to support its development.

The set of differential equations describing the mass transport in the various compartments is provided in Appendix 1. The model was coded using Advanced Continuous Simulation Language (ACSL) for Windows (Pharsight, Palo Alto, CA), a software developed to simulate the behavior of complex dynamical systems. The entire PK model coded using ACSL is also provided in Appendix 1. A brief description of the model parameterization and model results is provided in the next section.

Model parameterization. A preliminary PK model was developed using the plasma concentration time course data for a single dose of MK-0679.

The challenge faced in the development of this model was the simultaneous fitting of a large number of model parameters from a relatively limited set of data. Ideally, many of these parameters would be set on the basis of other

experimental data. For example, the rate constant for clearance from the TB region could be inferred from data on the rate of transport of insoluble materials on the mucociliary ladder. Similarly, the rate constant for systemic uptake from the pulmonary region could be estimated from data on the rate of dissolution of the aerosol of interest in a physiological fluid. However, for the purpose of this initial investigation, all the parameters in the model had to be estimated strictly from the experimental PK data that had been provided.

The approach developed to overcome this simultaneous parameterization problem is a sequential estimate-and-fix method. In order to apply this approach, the various data sets available for fitting the model were ordered in a nested series, where all the parameters estimated with a previous data set in the series are held fixed during fitting of the next data set. Using this approach, the most basic PK data (the iv data) were modeled first, and the parameter set influencing the behavior of the model for this data was estimated. The next most basic data (the po data) were then modeled, and those parameters that had been estimated previously (with the iv data) were held fixed at the iv values. The data from the other routes of administration (in and it) were then modeled, holding the parameters estimated for the iv and po data fixed.

The model was used to predict the plasma levels following administration via the po, iv, in, and it routes and to illustrate how the systemic exposure could be predicted following a 1-h exposure to a hypothetical aerosol.

RESULTS

Route Comparison Study

Plasma concentrations of MK-0679. The area under the curve ($AUC_{0\text{-}6h}$), peak plasma concentration (C_{max}), time to reach peak plasma concentration (T_{max}), and plasma half-life ($t_{1/2}$) of MK-0679 following iv, po, it, or in administration are shown as absolute values and values normalized to dose in Table 1. Dose-normalized $AUC_{0\text{-}6h}$ and C_{max} were not significantly different between the po and in routes or between the iv and it routes following administration of MK-0679. However, dose-normalized $AUC_{0\text{-}6h}$ and C_{max} were significantly different between the iv and it routes compared with those of the po and in routes of exposure. Both the T_{max} and $t_{1/2}$ were comparable between iv and it routes of exposure. The T_{max} and $t_{1/2}$ following in administration were shorter compared with those following po administration of MK-0679 (Table 1). Dose-normalized mean plasma concentrations ($ng{\cdot}ml^{-1}/mg{\cdot}kg^{-1}$) of MK-0679 at 0–6 h post-dose for each route of administration are shown in Figure 2.

BAL and NL. Three animals/group were examined with the exception of one group in the BAL experiment and one group in the NL experiment when only two animals per group were examined due to dosing error or loss of sample. Due to limited sample size, therefore, statistical analyses were not performed. However, it appeared that a time-dependent inflammatory response, measured by increased total protein content in lavage fluid and percent polymorphonuclear cells, was induced in both the lower respiratory tract (LRT) and the nasal cavity following administration of MK-0679, especially at the 24-h post-it instillation time point. This is consistent with the observation of severe ocular irritation with this compound (data not shown) and the microscopic changes observed (see following).

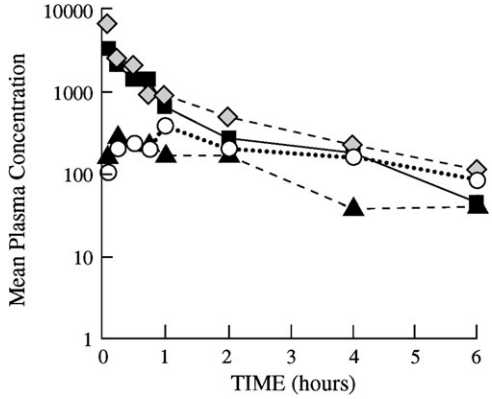

FIG. 2. Dose-normalized mean plasma concentrations ($ng{\cdot}ml^{-1}/mg{\cdot}kg^{-1}$) of MK-0679 for 0–6 h after administration of drug by the iv, it, po, and in routes.

Microscopic examination of lung tissue. Intratracheal instillation of MK-0679 caused a mild pneumonia with fibrin exudation in two of three rats at 24 h following instillation when compared with concurrent controls. The inflammatory lesions occupied 10% or less of the total lung parenchyma and were centered around the tertiary and terminal bronchioles and the alveoli. The inflammatory infiltrate pooled in alveolar spaces and consisted of approximately equal numbers of neutrophils and macrophages. Alveolar spaces were slightly thickened by hyperplastic pnuemocytes. Necrosis was not observed. Lungs examined at the 4-h time point after the instillation of MK-0679, as well as the vehicle and naive controls, were unremarkable.

Calculation of bioavailability for each route of administration. The equation used to calculate the bioavailability of MK-0679 following po, iv, in, and it administration is shown below.

$$F_{ROUTE} = \frac{Dose_{iv}}{Dose_{ROUTE}} \times \frac{AUC_{ROUTE}}{AUC_{iv}} \times 100,$$

where F_{ROUTE} is the percent bioavailability by the in (F_{in}), it (F_{it}), po (F_{po}), or iv (F_{iv}) route; and dose or AUC_{ROUTE} the dose or AUC of the route to be compared with the reference iv route.

Using the data in Table 1, the percent bioavailability via the po, in, and it routes were estimated to be 41.0, 24.7, and 138%, respectively. The latter exceeds the theoretical maximum of 100% (i.e., equivalent to iv) possibly due to slight differences in the time the first blood samples were taken following it exposure when the decreases in plasma concentrations were the greatest. In other words, due to the rapid decline in plasma levels following administration and distribution, the peak for iv was missed because it is theoretically impossible for other routes (e.g., it) to have higher peak plasma concentrations higher than iv.

Derivation of a BCF

The BCF shown in the denominator of the general equation used to derive OELs below is intended to permit adjustments for differences in bioavailability between the inhalation route and the clinical route (typically po or iv) from which the NOAEL was derived. Background on the use of BCF (absorption; also designated as α, which is defined as 1/*F*) and uncertainty factors used to establish OELs for active pharmaceutical ingredients is provided by Naumann and Weideman (1995).

General method for setting OELs:

$$\mathrm{OEL}\left(\mathrm{mg/m^3}\right) = \frac{(\mathrm{NOAEL})\,(\mathrm{BW})}{(\mathrm{UF_C})\,(\mathrm{MF})\,(V)\,(S)\,(\mathrm{BCF})},$$

where NOAEL is in mg/kg, BW in kg, UF_C the uncertainty factor (composite), MF the modifying factor, *V* the volume of air breathed by a worker in an 8-h day (m^3), and *S* the steady-state adjustment factor.

Two hypothetical scenarios are presented below to illustrate how a BCF could be used to adjust the OEL derived for MK-0679, where the critical effect was derived from po or iv studies. In each scenario, different hypothetical assumptions were made regarding particle size to show how the adjustment would change depending on the predominant site of deposition (and presumed absorption). We first assumed exposure was to aerosols of the bulk API with an MMAD of 10 μm. Secondly, we assumed exposure to aerosols from a pharmaceutical granulation formulation (containing the API) with an MMAD of 50 μm. According to the ACGIH (2008), in humans, particles with an MMAD of 10 μm are expected to deposit in approximately equal proportions in the URT (ET) and LRT (TB and PU) regions. Particles with an MMAD of 50 μm are expected to deposit almost exclusively in the URT, i.e., the nasopharyngeal region.

BCF for use with po data. The following equation was used to derive a BCF to adjust an OEL of 0.1 mg/m^3 for MK-0679 based on po data.

$$\mathrm{BCF} = \frac{d_{\mathrm{in}}F_{\mathrm{in}} + d_{\mathrm{it}}F_{\mathrm{it}}}{F_{\mathrm{po}}},$$

where *F* is the percent bioavailability by the in (F_{in}), it (F_{it}), po (F_{po}) route and *d* the fraction deposited in the URT (d_{in}) and LRT (d_{it}; assumes rate of absorption >> rate of respiratory tract clearance).

For a particle size of 10 μm, deposition occurs evenly between the ET and thoracic/PU regions, i.e., $d_{in} \cong 0.5$ (50%) and $d_{it} \cong 0.5$ (50%). For an aerosol with a particle size of 50 μm, it is assumed that 100% of the aerosol would deposit in the nasal (ET) region and none of the aerosol would reach the TB and deep lung (thoracic and PU) regions. Therefore, it is assumed that $d_{in} \cong 1$ (100%) and $d_{it} \cong 0$.

Using the equations above and the po, in, and it bioavailability data for MK-0679, the OEL of 0.1 mg/m^3 was adjusted downward by a factor of 2 for 10-μm particles and adjusted upward by a factor of 1.7 for 50-μm particles. The calculations are shown below:

For a particle size of 10 μm:

$$\mathrm{BCF} = \frac{(0.5)\,(24.7) + (0.5)\,(138.1)}{41.0} = 2.0.$$

Therefore,

$$\mathrm{OEL_{adjusted}} = \frac{\mathrm{OEL}}{\mathrm{BCF}} = \frac{\mathrm{OEL}}{2.0} = 0.05\,\mathrm{mg/m^3}.$$

For a particle size of 50 μm:

$$\mathrm{BCF} = \frac{(1)\,(24.7) + (0)\,(138.1)}{41.0} = 0.60.$$

Therefore,

$$\mathrm{OEL_{adjusted}} = \frac{\mathrm{OEL}}{\mathrm{BCF}} = \frac{\mathrm{OEL}}{0.6} = 0.17\,\mathrm{mg/m^3}.$$

BCF for use with iv data. The following equation would have been used to derive a BCF to adjust an OEL of 0.1 mg/m^3 for MK-0679 that was hypothetically established using iv data.

$$\mathrm{BCF} = \frac{d_{\mathrm{in}}F_{\mathrm{in}} + d_{\mathrm{it}}F_{\mathrm{it}}}{F_{\mathrm{iv}}} d_{\mathrm{in}}F_{\mathrm{in}} + d_{\mathrm{it}}F_{\mathrm{it}},$$

where *F* is the bioavailability by the in (F_{in}), it (F_{it}), or iv (F_{iv}) route and *d* the fraction deposited in the URT (d_{in}) and LRT (d_{it}; assumes rate of absorption >> rate of respiratory tract clearance).

In this case, the relative bioavailability term in the denominator for iv administration (by definition) is 100%. Deposition for each particle size category was apportioned the same as described above. In this case, for smaller particles (e.g., 10 μm), the OEL would be adjusted slightly upward using a BCF of 0.81 ($OEL_{adjusted}$ = 0.12 mg/m^3) to reflect the combined effect of partial nasal absorption and essentially complete absorption from the LRT. The OEL for large sizes (50 μm) would be adjusted upward by a factor of 4 with a BCF of 0.25 ($OEL_{adjusted}$ = 0.4 mg/m^3) reflecting the limited (25%) in bioavailability (absorption is assumed to be rapid compared with mucociliary clearance in the nasal region with subsequent swallowing and po absorption). The calculations are shown below:

For particle size of 10 μm:

$$\mathrm{BCF} = \frac{(0.5)\,(24.7) + (0.5)\,(138.1)}{100} = 0.81.$$

Therefore,

$$\mathrm{OEL}_{\mathrm{adjusted}} = \frac{\mathrm{OEL}}{\mathrm{BCF}} = \frac{\mathrm{OEL}}{0.81} = 0.12\,\mathrm{mg/m^3}.$$

For particle size of 50 μm:

$$\mathrm{BCF} = \frac{(1)\,(24.7) + (0)\,(138.1)}{100} = 0.25.$$

Therefore,

$$\mathrm{OEL}_{\mathrm{adjusted}} = \frac{\mathrm{OEL}}{\mathrm{BCF}} = \frac{\mathrm{OEL}}{0.25} = 0.4\,\mathrm{mg/m^3}.$$

PK Model Predictions

Figures 3 compares model simulations to the experimental data for the iv, po, in, and it dosing. It can be seen that a simple two-compartment description is adequate to capture the biphasic nature of the iv PK of the compound. The parameters that were adjusted to obtain this fit were those for clearance (VMAX and KM) and the transport rates into and out off the deep blood compartment (KIN and KOUT). In fact, VMAX and KM could not be independently identified because the iv data are consistent with linear kinetics. Both KIN and KOUT, on the other hand, could be uniquely identified from their differential impacts on the model behavior.

The ability of the resulting systemic model to reproduce the po data is also shown in Figure 3. The only parameters that were adjusted to obtain the observed fit were those for po absorption (KAGI) and fecal clearance (KCGI). The ability of the model to reproduce both the iv and the po data with the same systemic distribution and metabolism parameters demonstrates the utility of the sequential estimate-and-fix approach.

Figure 3 also shows the ability of the resulting systemic/GI absorption model to reproduce the data for in instillation. The only parameters that could be adjusted to attempt to fit the in data were the direct systemic uptake from the ET region (KAET) and the clearance from the ET region into the GI tract (KCET). It can be seen that the model uniformly overestimates the systemic uptake from the in route.

Finally, Figure 3 shows the ability of the same systemic/GI absorption model to reproduce the data for it instillation. It was necessary to estimate the fractional deposition in the TB and PU regions from the data for it dosing. There were five parameters that were nominally estimated from a single data set: fractional deposition in the TB region (FDTB) versus the PU region (FDPU = 1 − FDTB), as well as the systemic uptake and clearance from both the TB region (KATB and KCTB) and the PU region (KAPU and KCPU). In order to reduce the number of parameters that had to be estimated simultaneously, the physiological structures of the two regions were used to identify the key parameters in each region. The only parameters in the PU region that were estimated on the basis of the in data were the fractional deposition (FDPU) and

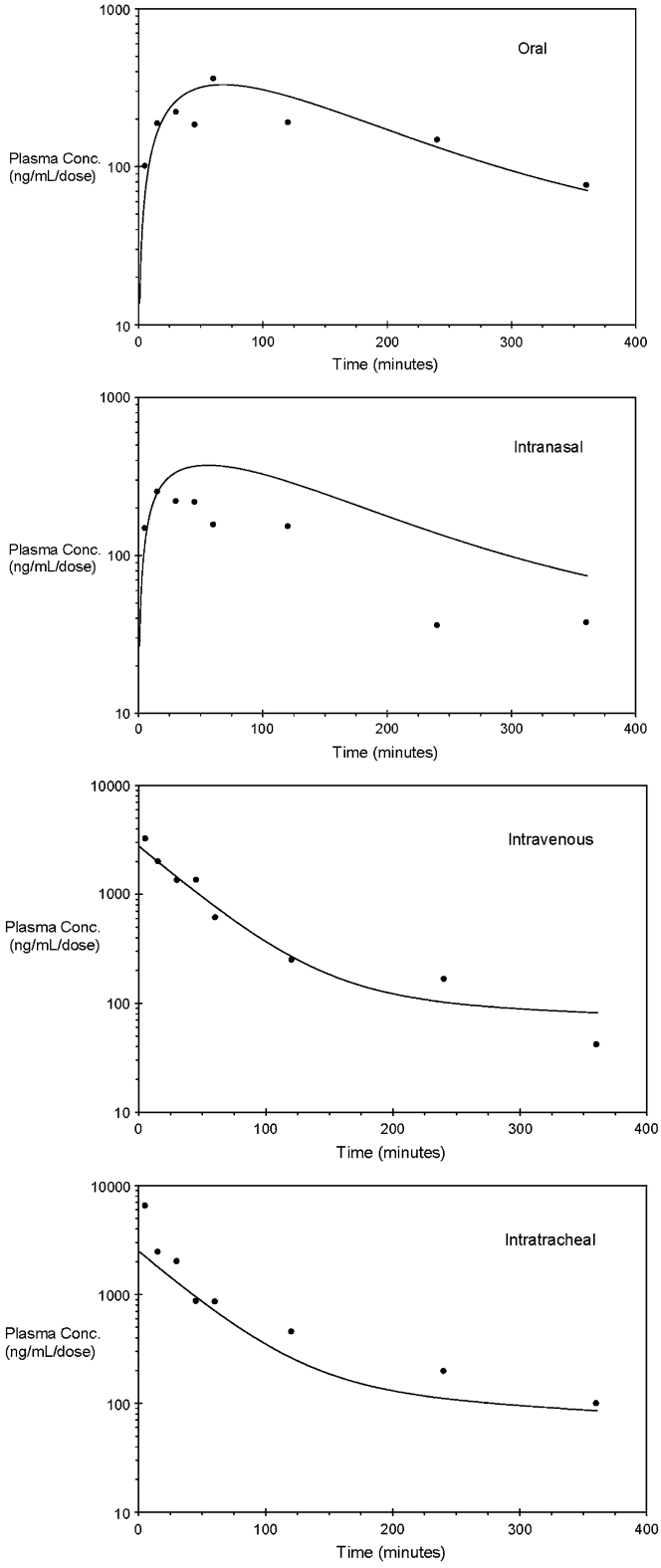

FIG. 3. Plots comparing experimentally measured plasma concentration time course to model predictions following iv, it, po, and in dosing in rats.

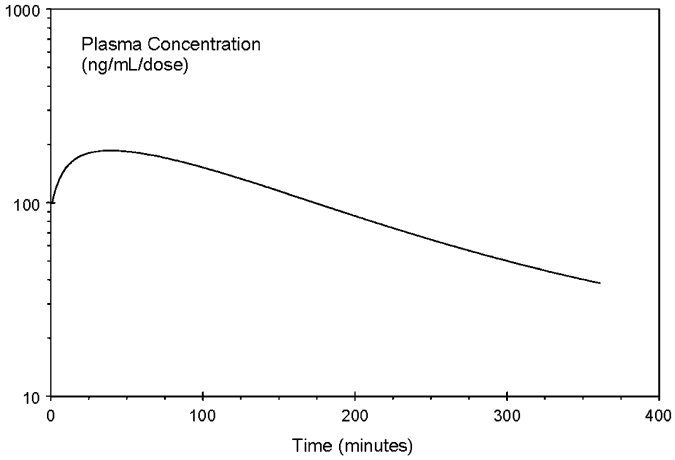

FIG. 4. Plot showing model derived plasma concentration time course in rats following inhalation of 1.3-μm aerosols. Fractional deposition in the respiratory tract compartments was calculated using the EPA (1994) particle dosimetry model.

TABLE 2
Summary of Parameters for the Inhalation PK Study Normalized for Exposure Dose

	Exposure group	
	1	2
MMAD (μm)	1.4	3.5
Exposure dose (mg/kg BW)	4.75	8.23
T_{max} (h)	1	1
$t_{1/2}$ (h)[a]	1.6	1.7
C_{max}/exposure dose ($ng \cdot ml^{-1}/mg \cdot kg^{-1}$)	224	175
$AUC^{b}_{0\text{-}6h}$/exposure dose ($ng \cdot h \cdot ml^{-1}/mg \cdot kg^{-1}$)	430	467

[a]Estimated based on a spline curve (SigmaPlot, version 8.0; SPSS, Inc.).
[b]Computed using the trapezoidal rule (SigmaPlot, version 8.0; SPSS, Inc.).

the rate of systemic uptake (KAPU). The only parameters in the TB region that were estimated on the basis of the it data were the fractional deposition (FDTB, which must be 1 − FDPU) and the rate of clearance to the GI tract (KCTB). The relatively unimportant parameters KCPU and KATB were set to an arbitrary small value (i.e., zero). The model underpredicted the systemic absorption from the lung slightly. However, the agreement of the model with the it data is surprisingly good given the simplicity of the model structure and provides encouragement that the simple approach described here may prove useful.

Figure 4 demonstrates how the model could be used to predict systemic uptake from an inhalation exposure. To create the plasma time course shown in this figure, the model was run with the set of parameters estimated from the four data sets: iv, po, in, and it. In this case, however, the fractional deposition in the lung regions (FDET = 0.4, FDTB = 0.05, and FDPU = 0.033) was calculated for a typical aerosol size (MMAD = 1.3 μm and GSD =2.5), using the EPA (1994) particle dosimetry model.

Inhalation PK Study

Delivered doses. The exposure parameters for the inhalation PK study are given in Table 2. The MMADs were 1.4 and 3.5 μm for exposure groups 1 and 2, respectively. The corresponding drug aerosol mass concentrations (mean ± SD) were 89 ± 10.9 and 164 ± 34.8 mg/m^3, and the calculated exposure dose levels (i.e., exposure dose) were 4.75 and 8.23 mg/kg BW, respectively. These values are not corrected for aerosol deposition efficiency.

Plasma concentrations. Postexposure PK parameters, including C_{max} and AUC values adjusted for the dose delivered to different respiratory tract regions, are given in Tables 2 and 3. The mean normalized plasma concentrations for exposure group 1 (i.e., Dp =1.4 μm) and exposure group 2 (i.e., Dp = 3.5 μm) are shown in Figure 5. The overall systemic absorption and time course for plasma concentrations of MK-0679 following inhalation exposure of aerosol particles of 1.4- and 3.5-μm MMADs were similar. For both particle sizes, postexposure plasma drug levels increased initially, reached to C_{max} at approximately 1 h postexposure, decreased rapidly to less than 40% of C_{max} at 2 h postexposure, and gradually decreased to approximately 10–20% of C_{max} at 6 h postexposure. For direct comparisons, the deposition dose, C_{max}, and AUC values for the different parts of the respiratory tract, e.g., ET and lung (TB + PU), are presented separately in Table 3.

DISCUSSION

The experiments/evaluations described in this article were designed to show different approaches for defining the systemic exposure to soluble dusts following deposition in different parts of the respiratory tract. Although OELs for pharmaceuticals are based on a rich preclinical and clinical database, which permits a comprehensive evaluation of the inherent pharmacological and toxicological properties of the compound, the final extrapolation to a safe level of exposure following inhalation of pharmaceutical dusts in the workplace can introduce significant uncertainties. These investigations were intended to identify ways to reduce key uncertainties by collecting additional limited data and/or by employing simple models to better define systemic bioavailability following inhalation exposure.

Although it is important to consider route-related differences in bioavailability when setting OELs, it may be premature to use the experimental approach described in this article without further investigation. A number of assumptions were made in

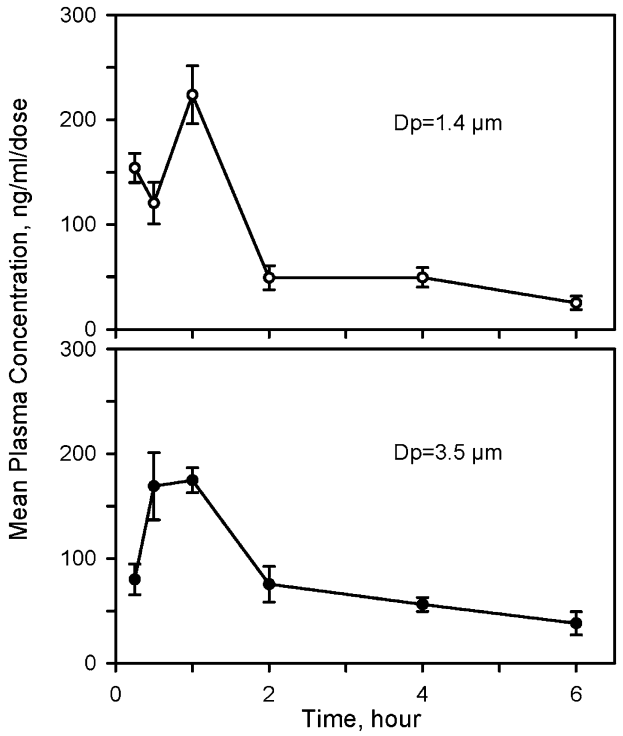

FIG. 5. Time course for plasma concentrations following inhalation of MK-0679 aerosols. Values are presented as means ± SE adjusted for exposure dose.

TABLE 3
Data Summary for the Inhalation PK Study. PK Parameters Were Adjusted for Regional Delivered Dose

	Exposure group	
	1	2
MMAD (µm)	1.4	3.5
Total delivered dose[a]		
Total dose (mg/kg)	1.71	7.00
C_{max}/total dose (ng·ml^{-1}/mg·kg^{-1})	621	205
$AUC^{b}_{0\text{-}6h}$/total dose (ng·h·ml^{-1}/mg·kg^{-1})	1193	550
ET		
Deposition dose[a] (mg/kg)	1.05	6.01
C_{max}/$Dose_{ET}$ (ng·ml^{-1}/mg·kg^{-1})	1012	239
$AUC^{b}_{0\text{-}6h}$/$Dose_{ET}$ (ng·h·ml^{-1}/mg·kg^{-1})	1943	640
Lung (TB + P)		
Deposition dose[a] (mg/kg)	0.67	0.99
C_{max}/$Dose_{LUNG}$ (ng·ml^{-1}/mg·kg^{-1})	1597	1454
$AUC^{b}_{0\text{-}6h}$/$Dose_{LUNG}$ (ng·h·ml^{-1}/mg·kg^{-1})	3068	3895

[a]Total dose, $Dose_{ET}$, and $Dose_{LUNG}$ (TB + P) were estimated based upon exposure dose and regional deposition fraction.
[b]Computed using the trapezoidal rule (SigmaPlot, version 8.0; SPSS, Inc.).

the rather simplistic application of the bioavailability data for calculation of absorption adjustment factors. For example, particle sizes of 10 and 50 µm were used to show how a BCF could be derived. The particle size of a compound can vary in different stages of the manufacturing processes (e.g., prior to and after milling) and the distribution of what is airborne may differ from the bulk material due to settling of coarse particles and the greater residence time for fine particles. The actual particle size of the compound present in the workplace air (not necessarily the same as the bulk material) would be needed to predict how the deposition would be apportioned between the ET and the TB/PU regions. If size-selective sampling data are available to characterize the size distribution, available particle deposition models can be used to estimate the regional deposited dose (EPA, 1994; ICRP, 1994).

The experimental approach used in the present study uses empirical data generated in rats, which are then extrapolated to humans. Some major assumptions implicit in this approach are that bioavailability (reflecting both rates of absorption and clearance) is similar in both species, i.e., it is assumed that any material not rapidly absorbed would be cleared from different parts of the respiratory tract via similar mechanisms and at similar rates. Based on the literature, these are not unreasonable assumptions (Schanker *et al.*, 1986); however, they have not yet been investigated adequately to support the routine use of route-specific bioavailability data to adjust OELs.

The results of the inhalation bioavailability study were consistent with the route comparison study where a single dosage of MK-0679 was administered to the Sprague-Dawley rats via the iv, it, po, and in routes. As mentioned earlier, the systemic bioavailability of MK-0679 via iv and it administration was much higher than that via po and in routes: $AUC_{0\text{-}6h}$ were 2707 ± 219, 3740 ± 360, 1110 ± 170, and 669 ± 71 ng·h·ml^{-1}/mg·kg^{-1} via iv, it, po, and in administration, respectively. It is interesting to note that in a comparison of AUC via it administration with the AUC associated with thoracic deposition dose from the inhalation study (3068–3895 ng·h·ml^{-1}/mg·kg^{-1}), there is good agreement in systemic bioavailability via the it and inhalation routes. This further indicated that thoracic (TB + PU) deposition is the most important dose index to predict the systemic bioavailability of inhaled MK-0679 and suggests that the absorption efficiency of MK-0679 in the respiratory tract by inhalation exposure is comparable with that via it instillation.

Good agreement of $AUC_{0\text{-}6h}$ with respect to LRT deposition dose for both 1.4 and 3.5 µm size particles also supports the conclusion that thoracic (TB and PU) deposition is the most appropriate dose index to predict the systemic bioavailability of inhaled MK-0679. The normalized $AUC_{0\text{-}6h}$ corrected for deposition efficiency for 1.4 µm size particles was three times that for 3.5 µm size particles, indicating that absorption efficiency of MK-0679 in the respiratory tract following inhalation of 3.5 µm particles was much lower than following inhalation of 1.4 µm size particles. Hence, the smaller value of systemic bioavailability for 3.5 µm size particles with respect to total deposition dose was skewed due to the greater particle

deposition rate in the nose. The implication of this is that deposition dose in the nasopharyngeal region did not appear to be a major factor in determining bioavailability of inhaled MK-0679.

The results of the route comparison study also provided data to develop and begin validating and refining a preliminary PK model. The model developed combines a multicompartment description of the respiratory tract with a simple compartmental model of systemic uptake and clearance. This simple model was used to estimate the systemic bioavailability of a drug administered as an aerosol. The model structure is consistent with EPA's (1994) particulate dosimetry model but is extended to account for disposition (systemic uptake or clearance) of the inhaled aerosol. The model structure provides a framework for integrating information on the regional deposition, clearance, and absorption of inhaled aerosols and supports the calculation of a regional absorbed dose as a component of a whole body PBPK model, potentially providing a broader framework for making cross-species dose comparisons. The model described in this report incorporates multiple routes of administration and thus provides a means to conduct route-to-route extrapolation to estimate the BCFs for pharmaceutical compounds. This strength is offset by one of its major limitations, i.e., using a relatively limited data set from a study using a small number of animals to simultaneously fit a large number of model parameters.

The modeling approach developed in these investigations performed well for iv and po dosing. This should not be surprising, given that the model was parameterized to fit the experimental data. More importantly, this indicates that a simple two-compartment description with first-order uptake from the GI tract and saturable elimination from the plasma compartment is an adequate representation for the iv and po dosing routes for this chemical.

The modeling approach performed less well for the in dosing route. Specifically, it overpredicted the drug plasma concentration for in. This discrepancy probably indicates that the simple first-order absorption and clearance terms used in the nasal description is an inadequate representation. The absorption kinetics in the nose are quite complex and are influenced by a number of factors such as the site of deposition, solubility of the compound, dissolution rate of the aerosol formulation, tissue permeability, local metabolism, blood perfusion rate at the site of deposition in the nose, and relatively rapid rates of mucociliary clearance. Simple first-order absorption and clearance rates apparently are unable to account for the disposition and/or transport processes in the nasal compartment. The inhalation study suggested that ET absorption for this compound did not contribute significantly to systemic exposure.

The modeling approach was more successful in reproducing the it data, although it also underpredicted the experimental data to some extent. This may have been due to an overestimation of TB deposition or an underprediction of TB absorption. The latter seems to be supported by the results of the inhalation study. It should be understood, of course, that the purpose of this exercise was not to provide unequivocal results for the specific chemical modeled but was intended to demonstrate the viability of the concept. Based on the relatively successful outcome of this preliminary effort, there is good reason to believe that the basic approach described here (the sequential estimate-and-fix approach) can provide a generally useful tool for estimating systemic uptake (regional absorbed dose) for other chemicals. Refinements can be made in the future, e.g., using actual BWs rather than a fixed BW of 250 g, to improve accuracy of predictions.

There are, of course, other considerations that may be important for other chemicals. As a general consideration, the nasal mucosa and Clara cell–rich regions of the lung have a high degree of enzymatic activity that may result in a first-pass effect for metabolized drugs depositing at these sites in the respiratory tract. Other regions of the respiratory tract with low metabolic activity can act as depots for the inhaled drug and influence the time course of the plasma concentration depending on the lipid:blood partition coefficient for the compound and the regional blood perfusion rate. In the model development, we did not consider the metabolic activity and the storage capacity of the respiratory tract tissue. For in and it dosing, a limited sensitivity analysis using both the maximal plasma concentration and the area under the plasma concentration curve as the relevant dose metric indicates that the bioavailability depends more on the absorption rate than on the clearance rate in a given lung compartment. Hence, the collection of data to provide a more accurate representation of the transport kinetics in the nasal region and lung would improve the model prediction for these two dosing routes.

Another key assumption is that the in and it instillation of solutions simulates inhalation of soluble particles, both in terms of deposition pattern and rate of absorption. This issue is the subject of an ongoing debate. Within the narrow context of deposition and absorption of soluble aerosols, the use of instillation techniques in lieu of an inhalation bioavailability study may still be worthwhile pursuing. The inhalation bioavailability study with MK-0679 using similar blood sampling times was useful to validate the utility of instillation techniques to assess regional bioavailability for this compound. Further support for the general application of this approach could come from additional studies with other compounds, preferably with different physicochemical properties.

Historically, the bioavailability of inhaled substances has often been conservatively assumed to be 100%. Depending on the aerosol size, only a fraction of the inhaled particles are deposited in the airways (Sarangapani and Wexler, 1999). Furthermore, depending on the properties of the deposited aerosol, the clearance can differ between rodents and humans. Adjusting for these differences can significantly alter the BCF and thereby influence the OEL. Based on numerous experimental studies, empirical relations have been derived to

compute the regional deposited fraction for inhaled aerosols in the lung (EPA, 1994; ICRP, 1994; James *et al*., 1991). These deposition models need to be incorporated into PK models, such as the one described in this study, in order to predict the bioavailability of inhaled aerosols. The inhalation PK study was performed on MK-0679 to validate the model parameters derived from the multiroute comparison study. Successful modeling/validation of several materials in this way, spanning a range of physicochemical characteristics, could obviate the need to conduct inhalation experiments on rodents to determine the bioavailability of inhaled aerosols in the future.

The time, expense, and number of animals used to perform inhalation bioavailability studies may not be justified to support setting OELs for every compound. However, the evaluation of the fate of inhaled soluble aerosols of MK-0679 showed that surrogate testing (e.g., in and it instillation) could provide sufficient support for adjusting OELs of commercially important compounds. Sufficient details on the experimental and modeling methods employed are provided in this article to facilitate further development of these approaches by other investigators.

Recommendations for Future Investigations

Route comparison and companion inhalation PK studies should be conducted for additional compounds spanning a range of physicochemical properties (MW, water solubility, log K_{ow}) to determine how the findings of this study can be generalized across different categories of compounds. Sufficient methodological details were included here to facilitate these follow-up investigations.

The simple PK model to estimate drug plasma concentration following multiple routes of administration described in this report was an initial scoping effort to explore the feasibility of using a PK approach to estimate the regional bioavailability of administered drugs. Based on this initial work, the following areas of research on potential improvements are suggested.

First principles–based approach. An alternative or parallel strategy for validating the proposed modeling approach would be to base it on first principles. The bioavailability of inhaled substances depends on both the microenvironment at the site of deposition and the physicochemical properties of the deposited compound. The current model treats the respiratory tract as a "black box" and estimates the model parameters by fitting model derived plasma concentrations to the experimental data. This is a compound-specific and data-intensive approach, not easily amenable to model the bioavailability of a diverse group of inhaled aerosols. A more generic first principles–based lung model, where the transport processes are formulated based on physiological processes, needs to be developed. More specifically, the dissolution process in the airway fluid needs to be modeled. Simple *in vitro* dissolution experiments of aerosolized drugs in a saline solution (to simulate the mucous environment in the lung) can be conducted to determine dissolution rates and support model parameterization. Also, the airway permeability and transport across the epithelial tissue need to be modeled. Transport kinetics in the lung, although quite complex, has been well characterized in the literature (Overton, 1984; Schanker, 1978). For inhaled aerosols, Byron (1986) proposed a mathematical model to study the residence time of aerosolized drugs in different regions of the respiratory tract and predict their systemic availability as a function of time. Gonda (1988) extended this model by incorporating release kinetics of drugs from a carrier deposited in the respiratory tract and the clearance of the drug by mucociliary and nonmucociliary mechanisms. Respiratory tract uptake models for inhaled vapors have been developed and used extensively in risk assessment (Andersen *et al*., 1999). Similar models can be developed for inhaled aerosols. The current model is only the first step in this direction. Confidence in the first principles–based PK approach can be achieved by comparing model derived plasma concentration to experimental data from multiple test compounds with widely different chemical characteristics. Additional interroute comparison studies on compounds with well-defined physicochemical parameters could lead to model parameterization based solely on physicochemical properties and first principles.

Modeling local tissue dose. For certain aerosols, it is desirable to estimate the dose to local tissues at or near the site of deposition. For example, Adamson *et al*. (1999) showed that the pulmonary toxicity of an atmospheric particulate sample was likely due to the metal ions that were readily leachable in the soluble fraction (15% of total). Gerde *et al*. (1994) showed that highly lipophilic compounds such as polycyclic aromatic hydrocarbons can accumulate in respiratory tract epithelium, increasing their local tissue concentration and slowing systemic absorption. This may be particularly important for drugs that act locally in the respiratory tract.

Whole body PK model. Plasma concentration is an extremely valuable measure of the dose, but under certain conditions, this may not be the most relevant dose metric for toxicity. PK models are flexible tools to study various dose measures at different sites in the body. In addition to estimating dosimetric adjustment factors and BCFs, such biologically based PK models can be used for interspecies dose extrapolation and to study the effect of interindividual variability on appropriate target tissue dose. Knowledge of the key factors that determine interindividual or interspecies differences in regional absorbed dose could provide the basis for collection of experimental data to support categorical data-derived or chemical-specific adjustment factors to replace default uncertainty factors. Models describing regional absorbed dose can complement other research designed to enhance understanding of bioavailability of compounds, their translocation to tissue and extrapulmonary compartments, and the role of TB and alveolar clearance mechanisms. Differences in regional absorbed dose may also improve our understanding of dosimetry-based mechanisms for the increased incidence of adverse health outcomes in susceptible subpopulations. These

models may have application in new drug development or in the assessment of occupational and environmental health risks.

FUNDING

Merck & Co., Inc. (four-route comparison and inhalation studies); American Industrial Health Council (model development).

ACKNOWLEDGMENTS

The authors extend their appreciation to Justine Thomas and Beverly Shelton for assisting with the route comparison study, to Darryl Patrick for performing the histopathological evaluations of lung tissue, and to Harvey Clewell, Robinan Gentry, and Annie Jarabek for guidance on PK model development. The PK model described in this report was developed by ICF Kaiser for the American Industrial Health Council, Dosimetry and Risk Assessment Subcommittee under the direction of Clay Frederick and Matt Bogdanffy. Special thanks are also given to Greg Kedderis for reviewing and providing insightful comments on the manuscript.

APPENDIX 1

Differential Mass Balance Equations in the Various Compartments

$$\text{ET compartment}: \frac{dM_{et}}{dt} = -K_{et}^{A}M_{et} - K_{et}^{C}M_{et}$$

$$\text{TB compartment}: \frac{dM_{tb}}{dt} = -K_{tb}^{A}M_{tb} - K_{tb}^{C}M_{tb} + K_{pu}^{C}M_{pu}$$

$$\text{PU compartment}: \frac{dM_{pu}}{dt} = -K_{pu}^{A}M_{pu} - K_{pu}^{C}M_{pu}$$

$$\text{GI compartment}: \frac{dM_{gi}}{dt} = -K_{et}^{C}M_{et} + K_{tb}^{C}M_{tb} - K_{gi}^{A}M_{gi} - K_{gi}^{C}M_{gi}$$

$$\text{Plasma compartment}: \frac{dM_{p}}{dt} = K_{et}^{A}M_{et} + K_{tb}^{A}M_{tb} + K_{pu}^{A}M_{pu} + K_{gi}^{A}M_{gi} - \frac{V_m\left(M_p/\mathrm{VD}\right)}{K_m + M_p/\mathrm{VD}} - K_{out}M_p + K_{in}M_{dp}$$

$$\text{Deep plasma compartment}: \frac{dM_{dp}}{dt} = K_{out}M_p - K_{in}M_{dp}$$

where K_i^A are the first-order absorption rates in the various compartments, K_i^C are the first-order clearance rates in the various compartments, V_m and K_m are the kinetic parameters for systemic elimination, and VD is the volume of distribution.

MULTIROUTE DRUG DISPOSITION PK MODEL CSL FILE

Initial Program

```
CONSTANT BW = 0.25          $'Body Weight (kg)'
CONSTANT DOSE = 12.5        $'Inhaled dose (mg/kg)'
CONSTANT FDET = 0.          $'Fractional Deposition in ET region'
CONSTANT FDTB = 0.6         $'Fractional Deposition in TB region'
CONSTANT FDPU = 0.4         $'Fractional Deposition in PU region'
CONSTANT FDGI = 0.          $'Fraction of Dose Direct to GI Tract'
CONSTANT FDPL = 0.          $'Fraction of Dose Direct to Plasma'

IDOSE = DOSE*BW
DDET = FDET*IDOSE           $'initial dose to ET region'
DDTB = FDTB*IDOSE           $'initial dose to TB region'
DDPU = FDPU*IDOSE           $'initial dose to PU region'
DDGI = FDGI*IDOSE           $'initial dose to GI tract'
DDPL = FDPL*IDOSE           $'initial dose to plasma'

CONSTANT KAET = 0.01        $'1st order absorption rate cont. in ET (/min)'
CONSTANT KATB = 0.          $'1st order absorption rate cont. in TB (/min)'
CONSTANT KAPU = 10.         $'1st order absorption rate cont. in PU (/min)'
CONSTANT KAGI = 0.005       $'1st order absorption rate cont. in GI (/min)'
CONSTANT KCET = 0.1         $'1st order clearance rate in ET (/min)'
CONSTANT KCTB = 0.01        $'1st order clearance rate in TB (/min)'
CONSTANT KCPU = 0.          $'1st order clearance rate in PU (/min)'
CONSTANT KCGI = 0.005       $'1st order clearance rate in GI (/min)'
CONSTANT KD = 0.01          $'1st order rate constant into deep compartment'
CONSTANT KR = 0.002         $'1st order rate constant from deep compartment'
CONSTANT VMAX = 110.        $'km for elimination from blood (mg/min)'
CONSTANT KM = 100.          $'Vmax for elimination from blood (mg/ml)'
CONSTANT VD = 90.           $'Volume of distribution (ml)'

CONSTANT TSTOP = 360.
CINT = 1.0
VARIABLE TIME
ALGORITHM IALG = 2

END
DYNAMIC
DERIVATIVE
RMET = -KAET*MET            $'mass balance ET comp.'
   - KCET*MET
MET = INTEG(RMET, DDET)

RMTB = -KATB*MTB            $'mass balance TB comp.'
   - KCTB*MTB
   + KCPU*MPU
MTB = INTEG(RMTB, DDTB)

RMPU = -KAPU*MPU            $'mass balance PU comp.'
   - KCPU*MPU
MPU = INTEG(RMPU, DDPU)
RMGI = KCET*MET             $'mass balance GI comp.'
   + KCTB*MTB
   - KAGI*MGI - KCGI*MGI
MGI = INTEG(RMGI, DDGI)

RMF = KCGI*MGI              $'elimination to feces'
MF = INTEG(RMF, 0.0)

RMPLAS = KAET*MET           $'mass balance Plasma'
   + KATB*MTB
   + KAPU*MPU
```

```
  +KAGI*MGI − VMAX*CPLAS/
  (KM + CPLAS)
  −KIN*MPLAS + KOUT*MDEEP
MPLAS = INTEG(RMPLAS, DDPL)
CPLAS = MPLAS/VD
AUCP = INTEG(CPLAS, 0.0)
NCPLAS = 1.0E6*CPLAS/DOSE
NAUCP = INTEG(NCPLAS, 0.0)

RMCL = VMAX*CPLAS/(KM + CPLAS)
MCL = INTEG(RMCL, 0.0)

RMDEEP = KIN*MPLAS − KOUT*MDEEP
MDEEP = INTEG(RMDEEP, 0.0)
TM = MET + MTB + MPU + MGI + MF + MPLAS + MCL + MDEEP
MBAL = TM – IDOSE          $'overall mass balance'
TERMT(TIME.gt.TSTOP)

END $'of DERIVATIVE'
END $'of DYNAMIC'
END $'of PROGRAM'

prepare 'all'

PROCED rat
s kcet=0.1 kctb=0.01 kcpu=0.0 kcgi=0.005 vmax=110.0
s kaet=0.01 katb=0.0 kapu=10.0 kagi=0.005 km=100.0
s kd=.01 kr=.002
s bw=0.25 vd=90.0
END

PROCED piv
S DOSE=10. FDET=0. FDTB=0. FDPU=0. FDGI=0. FDPL=1.
start
PLOT /DATA=IV /log /hi=10000. /lo=10. /xhi=400...
/xlo=0. NCPLAS /XTAG='−Time (min)'...
/TAG='IV dosing − Plasma Conc (ng/ml/mg/kg)'
END

PROCED por
S DOSE=100 FDET=0. FDTB=0. FDPU=0. FDGI=1. FDPL=0.
start
PLOT /DATA=OR /log /hi=1000. /lo=10. /xhi=400...
/xlo=0. NCPLAS /XTAG='−Time (min)'...
/TAG='OR dosing − Plasma Conc (ng/ml/mg/kg)'
END

PROCED pit
S DOSE=12.5 FDET=0. FDTB=0.15 FDPU=0.85 FDGI=0. FDPL=0.
start
PLOT /DATA=IT /log /hi=10000. /lo=10. /xhi=400...
/xlo=0. NCPLAS /XTAG='−Time (min)'...
/TAG='IT dosing − Plasma Conc (ng/ml/mg/kg)'
END

PROCED pin
S DOSE=12.5 FDET=0.9 FDTB=0.1 FDPU=0.0 FDGI=0. FDPL=0.
start
PLOT /DATA=IN /log /hi=1000. /lo=10. /xhi=400...
/xlo=0. NCPLAS /XTAG='−Time (min)'...
/TAG='IN dosing − Plasma Conc (ng/ml/mg/kg)'
END

PROCED pinh
S DOSE=12.5 FDET=0.4 FDTB=0.05 FDPU=0.033 FDGI=0. FDPL=0.
start
PLOT /log /hi=10000. /lo=10. /xhi=400...
/xlo=0. NCPLAS /XTAG='−Time (min)'...
/TAG='Inhalation − Plasma Conc (ng/ml/mg/kg)'
END

DATA IV (TIME, NCPLAS)
5.00 3266.238
15.0 2018.731
30.0 1355.446
45.0 1362.798
60.0 616.872
120. 251.491
240. 167.917
360. 42.091
END

DATA OR (TIME, NCPLAS)
5.00 101.526
15.0 188.390
30.0 222.604
45.0 185.082
60.0 362.308
120. 190.771
240. 148.550
360. 76.718
END

DATA IT (TIME, NCPLAS)
5.00 6563.093
15.0 2472.922
30.0 2027.543
45.0 875.756
60.0 863.803
120. 457.252
240. 198.798
360. 100.569
END

DATA IN (TIME, NCPLAS)
5.00 149.335
15.0 254.268
30.0 221.584
45.0 218.665
60.0 157.297
120. 153.634
240. 36.208
360. 37.784
END

S WESITG=.F. FTSPLT=.T.
DATA IN (TIME, NCPLAS)
```

REFERENCES

Adamson, I. Y. E., Prieditis, H., and Vincent, R. (1999). Pulmonary toxicity of an atmospheric particulate sample is due to the soluble fraction. *Toxicol. Appl. Pharmacol.* **157,** 43–50.

American Conference of Governmental Industrial Hygienists (ACGIH). (2008). *2009 TLVs and BEIs Based on the Documentation of the Threshold Limit Values for Chemical Substances and Physical Agents and Biological Exposure Indices.* American Conference of Governmental Industrial Hygienists Cincinnati, OH.

Andersen, M. E., Green, T., Frederick, C. B., and Bogdanffy, M. S. (2002). Physiologically based pharmacokinetic (PBPK) models for nasal tissue dosimetry of organic esters: Assessing the state-of-knowledge and risk assessment applications with methyl methacrylate and vinyl acetate. *Regul. Toxicol. Pharmacol.* **36,** 234–245.

Andersen, M. E., Sarangapani, R., Gentry, P. R., Clewell, H. J., Covington, T. R., and Frederick, C. B. (2000). Application of a hybrid CFD-PBPK nasal

dosimetry model in an inhalation risk assessment: An example with acrylic acid. *Toxicol. Sci.* **57,** 312–325.

Andersen, M. E., Sarangapani, R., Frederick, C. B., and Kimbell, J. S. (1999). Dosimetric adjustment factors for methyl methacrylate derived from a steady-state analysis of a physiologically based clearance-extraction model. *Inhal. Toxicol.* **11,** 899–926.

Brown, R. J., and Schanker, L. (1983). Absorption of aerosolized drugs from the rat lung. *Drug Metab. Dispos.* **11,** 355–360.

Byron, P. (1986). Prediction of drug residence times in regions of the human respiratory tract following aerosol inhalation. *J. Pharm. Sci.* **75,** 433–438.

Environmental Protection Agency (EPA). (1994, October). *Methods for Derivation of Inhalation Reference Concentrations and Application of Inhalation Dosimetry*. EPA/600/8–90/066F. U.S. EPA, Office of Research and Development, Washington, DC.

Gerde, P., Muggenburg, B. A., Hoover, M. D., and Henderson, R. F. (1994). Clearance of particles and lipophilic solutes from central airways. *Ann. Occup. Hyg.* **38**(Suppl. 1), 211–214.

Gonda, I. (1988). Drugs administered directly into the respiratory tract: Modeling of the duration of effective drug levels. *J. Pharm. Sci.* **77,** 340–356.

Gopalakrishnan, M., Suarez, S., Hickey, A. J., and Gobburu, J. V. (2005). Population pharmacokinetic-pharmacodynamic modeling of subcutaneous and pulmonary insulin in rats. *J. Pharmacokinet. Pharmacodyn.* **32,** 485–500.

Hinchcliffe, M., and Illum, L. (1999). Intranasal insulin delivery and therapy. *Adv. Drug Deliv. Rev.* **35,** 199–234.

Hsu, J. C. (1996). *Multiple Comparisons: Theory and Methods*, p. 14. Chapman and Hall, London.

International Commission on Radiological Protection. (ICRP). (1994). *Human Respiratory Tract Model for Radiological Protection: A Report of a Task Group of the International Commission on Radiological Protection* (Annals of the ICRP, publication #66, V24, nos. 1–3). Elsevier Sciences Ltd, Oxford, United Kingdom.

James, A., Stahlhofen, W., Rudolf, G., Egan, M., Nixon, W., Gehr, P., and Brian, K. (1991). The respiratory tract deposition model proposed by the ICRP task group. *Radiat. Protection Dosimetry* **38,** 159–165.

Krishnaswami, S., Hochhaus, G., Mollmann, H., Barth, J., and Derendorg, H. (2005). Interpretation of absorption rate data for inhaled fluticasone propionate obtained in compartmental pharmacokinetic modeling. *Int. J. Clin. Pharmacol. Ther.* **43,** 117–122.

Mercer, T. (1967). On the role of particle size in the dissolution of lung burdens. *Health Phys.* **13,** 1211–1221.

Morrow, P. (1973). Alveolar clearance of aerosols. *Arch. Int. Med.* **131,** 101–108.

Naumann, B. D., and Weideman, P. A. (1995). Scientific basis for uncertainty factors used to establish occupational exposure limits for pharmaceutical active ingredients. *Hum. Ecol. Risk Assess.* **1,** 590–613.

Overton, J., Jr. (1984). Physicochemical processes and the formulation of dosimetry models. *Jpn J. Toxicol. Environ. Health* **13,** 273–294.

Raabe, O. G., Al-Bayati, M. A., Teague, S. V., and Rasolt, A. (1988). Regional deposition of inhaled, monodisperse, coarse and fine particles in small laboratory animals. In *Inhaled Particles VI* (J. Dodgson, R. I. McCallum, M. R. Bailey, and D. R. Fisher, Eds.), pp. 53–63. Pergamon Press, Oxford, United Kingdom.

Raabe, O. G., Yeh, H. C., Newton, G. J., Phalen, R. F., and Velasquez, D. J. (1977). Deposition of inhaled monodisperse aerosols in small rodents. In *Inhaled Particles IV* (W. H. Walton, Ed.), pp. 3–20. Pergamon Press, Oxford, United Kingdom.

Roy, M. (1989). Lung clearance modeling on the basis of physiological and biological parameters. *Health Phys.* **57**(Suppl. 1), 255–262.

Sarangapani, R., and Wexler, A. S. (2000). The role of dispersion on particles deposition in the human airways. *Toxicol. Sci.* **54,** 229–236.

Sargent, E. V., and Kirk, G. D. (1988). Establishing airborne exposure control limits in the pharmaceutical industry. *Am. Ind. Hyg. Assoc. J.* **49,** 309–313.

Schanker, L. (1978). Drug absorption from the lung. *Biochem. Pharmacol.* **27,** 381–385.

Schanker, L., Mitchell, E., and Brown, R. J. (1986). Species comparison of drug absorption from the lung after aerosol inhalation or intratracheal injection. *Drug Metab. Dispos.* **14,** 79–88.

Scheuch, G., Kohlhaeufl, M. J., Brand, P., and Siekmeier, R. (2006). Clinical perspectives on pulmonary systemic and macromolecular delivery. *Adv. Drug Deliv. Rev.* **58,** 996–1008.

Weideman, P. A., Naumann, B. D., Shen, C. F., Thomas, J. M., Shelton, B. A., Dixit, R., and Sargent, E. V. (1997). The use of bioavailability data in setting occupational exposure limits. *Toxicologist* **36,** 169 (Abstract).

Widdicombe, J. (1998). Drug uptake from the airways and lungs. *Indian J. Physiol. Pharmacol.* **42,** 3–14.